

Electronic structure of ordered and disordered Fe₃Pt

Zs Major¹, S B Dugdale¹, T Jarlborg², E Bruno³, B Ginatempo³,
J B Staunton⁴ and J Poulter⁵

¹ H H Wills Physics Laboratory, University of Bristol, Tyndall Avenue, Bristol BS8 1TL, UK

² Département de Physique de la Matière Condensée, Université de Genève, 24 quai Ernest Ansermet, CH-1211 Genève 4, Switzerland

³ Dipartimento di Fisica and Unità INFN, Università di Messina, Salita Sperone 31, 98166 Messina, Italy

⁴ Department of Physics, University of Warwick, Coventry CV4 7AL, UK

⁵ Department of Mathematics, Faculty of Science, Mahidol University, Rama 6 Road, Bangkok 10400, Thailand

Received 2 April 2003

Published 19 May 2003

Online at stacks.iop.org/JPhysCM/15/3619

Abstract

The electronic structure of invar alloys (i.e. materials in which the near absence of thermal expansion is observed) has been the focus of much study, owing both to the technological applications of these materials and interest in the fundamental mechanism that is responsible for the effect. Here, calculations of the magnetic Compton profiles are presented for ordered and disordered Fe₃Pt alloys. Using linear muffin-tin orbital and KKR methods, the latter incorporating the coherent potential approximation to describe the substitutional disorder, the electronic band structure and measurable quantities such as the Fermi surface topology are presented.

1. Introduction

The near absence of thermal expansion in Fe–Ni alloys over a certain range of composition and temperature was first reported more than a century ago by Guillaume [1]. Other alloys, such as Fe–Pt, also exhibit this invariability of their dimensions under heating, the characteristic which led Guillaume to name these alloys ‘invar’. While the mechanism behind the invar effect is still a matter of debate, it is widely thought that the answer lies in the existence of two almost degenerate magnetic states. Weiss [2] proposed that there could exist two different magnetic states (one ferromagnetic and one non-magnetic) with almost the same energy but different volumes, and that the invar properties could be explained in terms of thermal excitation from the larger-volume magnetic state into the smaller-volume state. Electronic structure calculations [3] confirmed that the total energies of the low-spin/low-volume and high-spin/high-volume states were indeed energetically very close to one another, hence giving credence to the phenomenological theory of Weiss [2]. Other calculations have suggested that non-collinear alignments of magnetic moments are necessary for a proper theoretical

description of the anomalous magnetovolume properties (see, for example, [4] and [5]). Experimentally, however, this suggestion is not supported, since so far only collinear spin arrangements have been observed ([6]). Interest in the electronic structure of Fe₃Pt has been stimulated recently by the observation of large magnetostriction, and hence shape-memory-alloy properties [7].

Temperature-dependent photoemission measurements [8] on one such invar alloy, Fe₃Pt, indicated a difference between the high- and low-temperature spectra. Recently, Srajer *et al* [9] reported large changes in the electronic spin-density in momentum space as a function of temperature in the same Fe₃Pt alloy. This paper, which focuses on a series of calculations of the momentum densities in both the ordered and disordered phases of Fe–Pt in the invar regime, has been prompted by new magnetic Compton scattering results [10, 11].

Inoue and Shimizu [12] (using a tight-binding method) and Hasegawa [13] (using the augmented plane wave (APW) method) made the first calculations of the electronic structure of ordered Fe₃Pt. Later, Podgórný [14, 15], using a fixed-spin-moment approach within the linear muffin-tin orbital (LMTO) scheme, made a very comprehensive study of total energies of the various magnetic states of the ordered phases. Hayn and Drchal [16] have also made calculations using the tight-binding LMTO incorporating the coherent potential approximation (CPA) to study the disordered compositions. However, this is the first time that calculations have been presented for both ordered and disordered Fe₃Pt within the same computational framework.

In this work we use the LMTO and KKR methods (the latter including the CPA) to study the electronic structure by calculating the spin-dependent momentum distributions that can be observed in magnetic Compton scattering [17] experiments.

2. Computational method

At low temperatures, ordered Fe₃Pt adopts the face-centred tetragonal structure [18], but for comparison with the disordered alloy, calculations were performed in the Cu₃Au structure. The electronic structure for ordered Fe₃Pt is calculated using both the LMTO [19] (including the so-called combined correction terms) and the KKR [20] methods. Additionally, the electronic structure of disordered Fe_{0.75}Pt_{0.25} is calculated using the KKR method, within the coherent potential approximation (KKR-CPA) [20]. Both the LMTO and KKR-CPA codes are scalar relativistic, using the local spin density approximation to the exchange–correlation functional (see [21] and [22] respectively) and include s, p, d and f functions. The LMTO calculations employed the atomic sphere approximation (ASA), with the Pt and Fe spheres having equal Wigner–Seitz radii. The KKR and KKR-CPA calculations used muffin-tin, rather than ASA potentials. Self-consistency was achieved using 816 *k*-points within the irreducible wedge of the simple cubic Brillouin zone (BZ) in the LMTO case; for the KKR and KKR-CPA calculations, the mesh of *k*-points was adaptive and determined principally by the required integration tolerances [20].

In order to compare the calculations with experiment, the electron momentum density (EMD) was calculated from the self-consistently determined potential. The Compton profile (CP) is a one-dimensional projection of the EMD, $\rho(\mathbf{p})$, which is related to the electron wavefunctions $\psi_{k,j}(\mathbf{r})$. In cases where electron–electron correlation can be neglected, this relationship has the form

$$\rho(\mathbf{p}) = \sum_{\text{occ.},j,k} \left| \int d\mathbf{r} \psi_{k,j}(\mathbf{r}) \exp(-i\mathbf{p} \cdot \mathbf{r}) \right|^2, \quad (1)$$

where j is a band index and the summation is over all occupied states. The CP, $J(p_z)$, is a double integral over the EMD:

$$J(p_z) = \int \int \rho(\mathbf{p}) \, dp_x \, dp_y. \quad (2)$$

In a spin-polarized system, the total EMD is composed of (different) contributions from spin-up and spin-down electrons,

$$\rho(\mathbf{p}) = \rho_{\uparrow}(\mathbf{p}) + \rho_{\downarrow}(\mathbf{p}), \quad (3)$$

where $\rho_{\uparrow}(\rho_{\downarrow})$ represents the spin-up (spin-down) EMD. If a spin moment, μ_{spin} , exists, this can be expressed in terms of the difference in occupancy of the spin-up and spin-down bands, i.e.

$$\mu_{\text{spin}} = \int [\rho_{\uparrow}(\mathbf{p}) - \rho_{\downarrow}(\mathbf{p})] \, d\mathbf{p}. \quad (4)$$

This difference can be measured in a magnetic Compton experiment owing to the spin-dependent terms in the scattering cross-section for elliptically polarized radiation [17].

The EMD was calculated for ordered Fe₃Pt using the LMTO wavefunctions [23] evaluated at 343 k -points in conjunction with 3695 reciprocal lattice vectors. This was then integrated along the appropriate directions to produce the CP.

The EMD for the disordered Fe_{0.75}Pt_{0.25} was calculated within the KKR-CPA framework [24]. It should be noted that while the KKR-CPA self-consistent potential from which the momentum density of the disordered Fe_{0.75}Pt_{0.25} was calculated is scalar relativistic, the KKR momentum density code itself is non-relativistic.

3. Results and discussion

A series of self-consistent KKR and KKR-CPA calculations was made at different lattice constants in both the magnetic and non-magnetic cases. From a simple parabolic fit to the KKR-CPA total energy values as a function of lattice constant, the equilibrium lattice constants for the disordered system in the magnetic and non-magnetic phases were found to be 7.12 and 6.90 au respectively; experimentally, the lattice constant is found to be 7.05 au [25]. This compares with 6.90 au, obtained from the ferromagnetic CPA calculations of Hayn and Drchal [16]. The smaller equilibrium lattice constants within the ASA might be due to the less attractive potential of the itinerant p (and f) states, so that their positive contribution to the pressure will be relatively small.

The total energy difference between the magnetic and non-magnetic states is 15.7 mRyd; this is larger than the values obtained by Podgórný [15] in the ordered alloy (1.2 mRyd) and by Hayn and Drchal [16] in the disordered alloy (0.7 mRyd). However, it is similar to that obtained by Uhl *et al* [4] (~ 12 mRyd) for their non-relativistic calculations on the ordered alloy. The LMTO results have been published previously by Moroni and Jarlborg [26], who obtained a ferromagnetic equilibrium lattice constant of 6.83 au with a total energy of about 2 mRyd lower than in the non-magnetic case.

Concerning the differences in total energy obtained in the current study with respect to those of others, it should be noted that this quantity depends sensitively on a number of computational details chosen in each framework. The difference between the total energy in the magnetic and non-magnetic phase would be sensitive to the particular choice of parametrization for the exchange–correlation potential, numbers of k -points used in performing the BZ integrations, the inclusion of f states in the basis set, performing full-potential calculations, including all relativistic effects, and by the choice of linearization energies (which is inherent

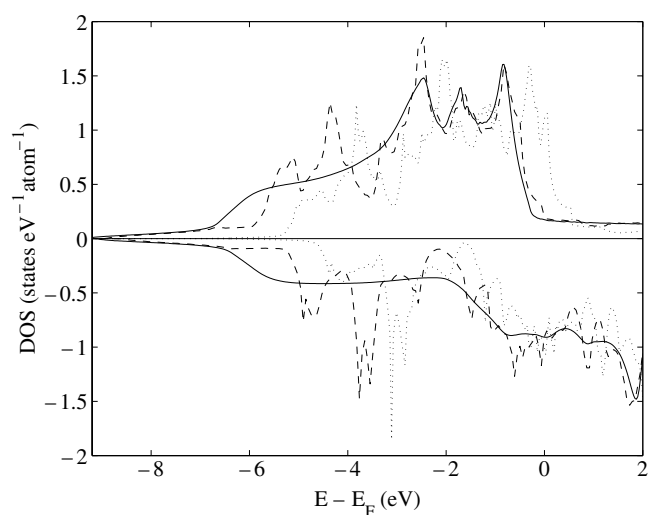


Figure 1. DOS for ordered Fe_3Pt from the KKR (dashed curve) and LMTO (dotted curve) calculations. The DOS for the disordered $\text{Fe}_{0.75}\text{Pt}_{0.25}$ calculated with the KKR-CPA method, is shown as the solid curve. The majority DOS is shown as positive, and the minority as negative.

to many calculational methods). The current calculations attempt as close a comparison as possible between the KKR and LMTO results in the ordered and disordered phases.

In order to be able to compare the results of the different calculations with each other and with experiment, all calculations presented in this paper were performed at the equilibrium lattice constant of the magnetic disordered phase (7.12 au).

The densities of states (DOS) for the three calculations are plotted in figure 1. For technical reasons in the KKR and KKR-CPA calculations, the DOS and band structures were evaluated with a small positive imaginary energy component of 1 mRyd. The DOS for $\text{Fe}_{0.75}\text{Pt}_{0.25}$ calculated within the KKR-CPA scheme is extremely smooth in comparison with the two calculations in the ordered phase due to the disorder that smears the electron states; we shall return to this point when we discuss the band structure. However, while the DOS is similar in all the calculations (and very similar except for a smoothing between the KKR and KKR-CPA calculations), there are differences at the Fermi level, particularly regarding the position of E_F relative to the d bands.

The LMTO and KKR band structures for ordered Fe_3Pt are plotted in figures 2 and 3 respectively. It can be seen that although the two are very similar, there are differences, particularly at the Fermi level. Thus the Fermi surface (FS) topologies predicted by the two calculations are qualitatively different. In particular, the LMTO predicts small (majority) hole pockets at Γ , whilst in the KKR band structure these bands are occupied at Γ . It can also be seen that the flat band along Γ -X just above the Fermi energy in the LMTO calculation appears below the Fermi energy in the KKR result. Spin-resolved angle-dependent photoemission experiments observed this flat majority band below the Fermi level [28]. For the minority bands, fewer differences exist. It is worth pointing out that the current LMTO results are almost identical to the previously published LMTO results of Podgórny [14], while the KKR bands are almost identical to the APW bands of Hasegawa [13].

Within the KKR method, the electron states are determined by the peaks in the Bloch spectral function (BSF) which is a function of energy and Bloch wavevector, \mathbf{k} [29]. In practice,

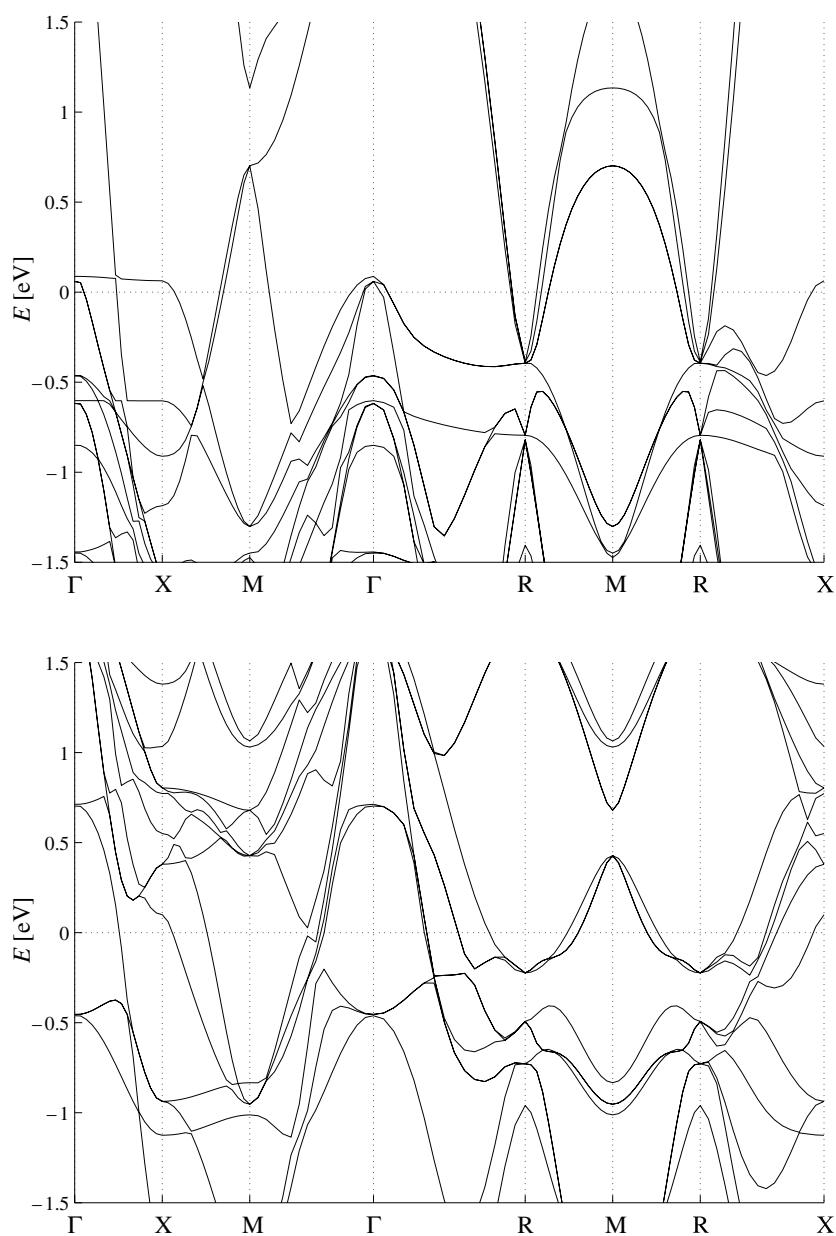


Figure 2. Majority (top) and minority (bottom) electron band structure of ordered Fe₃Pt from the LMTO calculations.

Lorentzian curves are fitted to the peaks in order to determine their position and width, the latter being a measure of the inverse lifetime of the state corresponding to that peak. In disordered systems where the lifetime of the electron states can be short, the peaks in the BSF broaden compared with the ordered case. At the Fermi level, the presence of broad peaks would mean that the FS is no longer 'sharp', and the derived spectral quantities, including the momentum distribution, would be similarly smeared.

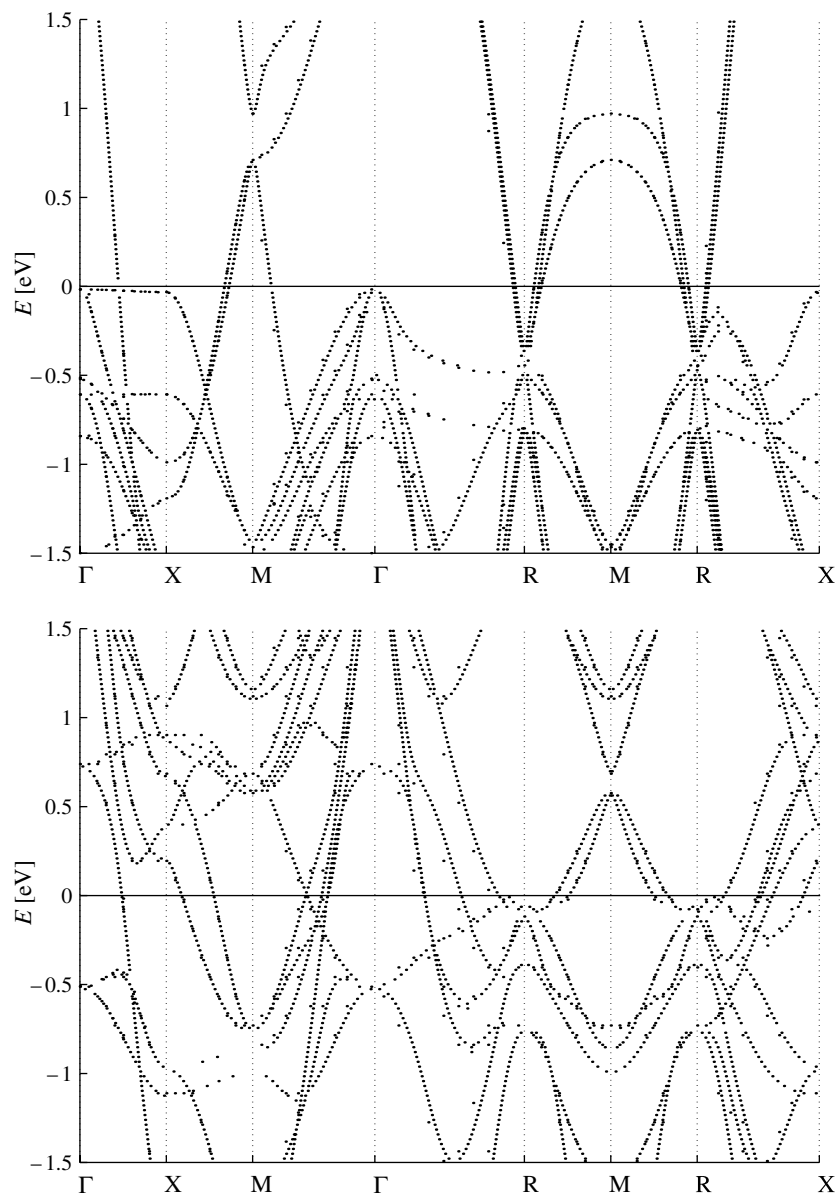


Figure 3. Majority (top) and minority (bottom) electron band structure of ordered Fe_3Pt from the KKR calculations.

There are small differences between the magnetic moments predicted for ordered Fe_3Pt (see table 1) by the LMTO and KKR methods, and it is evident that in the respective band structures the exchange splitting must be different (see figures 2 and 3).

The phonon softening [30] observed in this system could possibly be related to any FS nesting, but no experimental information exists on the FS topologies of either ordered Fe_3Pt or disordered $\text{Fe}_{0.75}\text{Pt}_{0.25}$. In the disordered case, traditional quantum oscillatory methods such as the measurement of the de Haas–van Alphen effect are excluded owing to the short electron

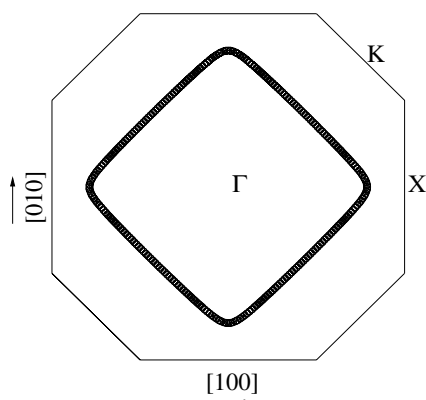


Figure 4. Majority FS of Fe_{0.75}Pt_{0.25} in the (001) plane from the KKR-CPA calculations. The first BZ is shown with some symmetry points marked.

Table 1. Magnetic moments obtained from the KKR, KKR-CPA and LMTO calculations, decomposed by site and angular momentum.

Method	Alloy	Moment (μ_B)								
		Fe s	Fe p	Fe d	Fe total	Pt s	Pt p	Pt d	Pt total	Total
KKR	Fe ₃ Pt	-0.009	-0.032	2.761	2.737	-0.038	-0.076	0.421	0.325	2.136
LMTO	Fe ₃ Pt	-0.003	-0.024	2.530	2.504	-0.027	-0.059	0.577	0.490	2.000
KKR-CPA	Fe _{0.75} Pt _{0.25}	-0.012	-0.040	2.836	2.799	-0.028	-0.056	0.302	0.227	2.156

mean-free paths. However, the FS could be revealed either by high-resolution Compton scattering or by two-dimensional angular correlation of electron-positron annihilation radiation (2D-ACAR) [31]. Wilkinson *et al* [31] recently presented the FS topology of the Cu_{1-x}Pd_x alloy system at certain compositions, revealing significant flat areas which are thought to nest and drive compositional ordering. In figure 4, a section through the majority FS of disordered Fe_{0.75}Pt_{0.25} is plotted in the (001) plane. While the DOS from the KKR-CPA calculation (figure 1) clearly shows the effect of smearing from the substitutional disorder, this sheet of FS is, in fact, reasonably well defined, since the widths of the BSF peaks at the Fermi level are smaller than the size of the points mapping out the FS contour in figure 4. This majority FS is clearly flattened along the [110] direction, and has a remarkable similarity to the FS topology of the Cu-Pd alloy system [31].

Further experimental investigations using positron annihilation into whether similar flattening could be related to the softening of the TA₁ [110] phonon [30], would justify a full theoretical study (including temperature effects, for example as described by Lee *et al* [32]); such experiments are under way.

The magnetic moments decomposed by site and angular momentum are shown in table 1. It should be noted that the moments associated with the more delocalized s and p electrons of both the Fe and the Pt constituents are negatively polarized with respect to the more localized d electrons across all the calculations. Moreover, the total and site-decomposed moments are not particularly sensitive to either the calculational scheme or whether the system is ordered or disordered. The localized components of the magnetic moments for Fe ($2.03 \pm 0.02 \mu_B$) and Pt ($0.34 \pm 0.08 \mu_B$) were inferred from spin-polarized neutron diffraction measurements by

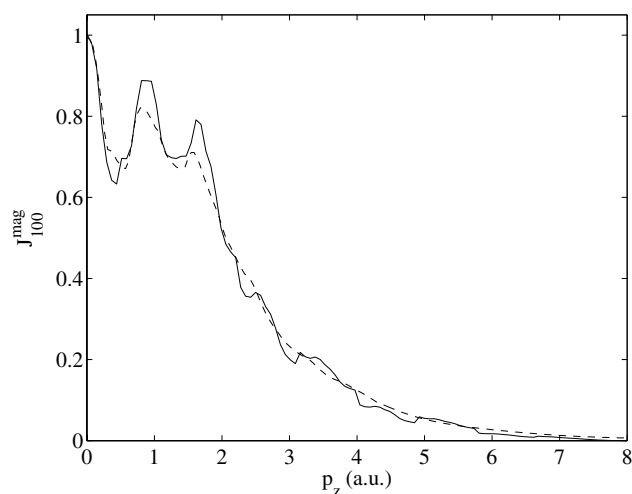


Figure 5. MCP along the [100] direction from the ordered LMTO (solid curve) and disordered KKR-CPA (dashed curve) calculations.

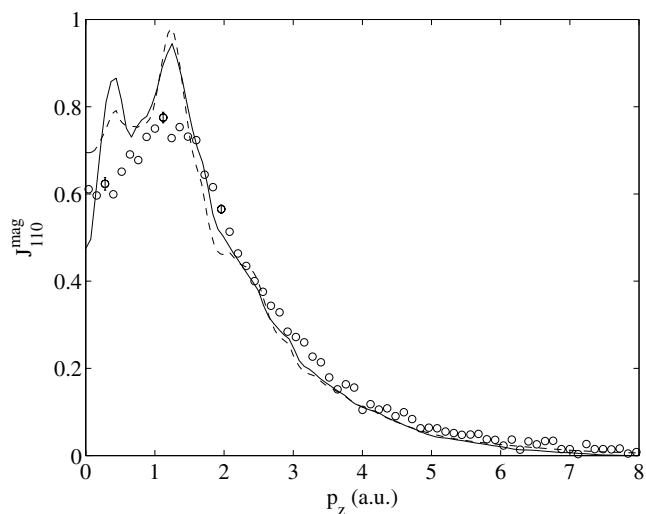


Figure 6. MCP along the [110] direction from the ordered LMTO (solid curve) and disordered KKR-CPA (dashed curve) calculations. The experimental data [10] for the disordered alloy are shown (open circles) with illustrative error bars. The calculations have not been convoluted with the experimental resolution function.

Ito *et al* [33], while the magnetization measurements of Caporaletti and Graham [34] indicated moments of 2.75 and $0.45 \mu_B$ for Fe and Pt respectively.

Magnetic Compton profiles (MCPs) have been extracted from the LMTO and the KKR-CPA calculations and are shown in figures 5, 6 and 7 for the [100], [110] and [111] directions respectively, alongside the experimental MCPs for the [110] and [111] directions in the disordered alloy obtained by Taylor *et al* [10]. None of the calculated profiles have been convoluted with the experimental resolution. In this way the main difference between the ordered and disordered profiles, that is to say that the disordered ones appear more smeared

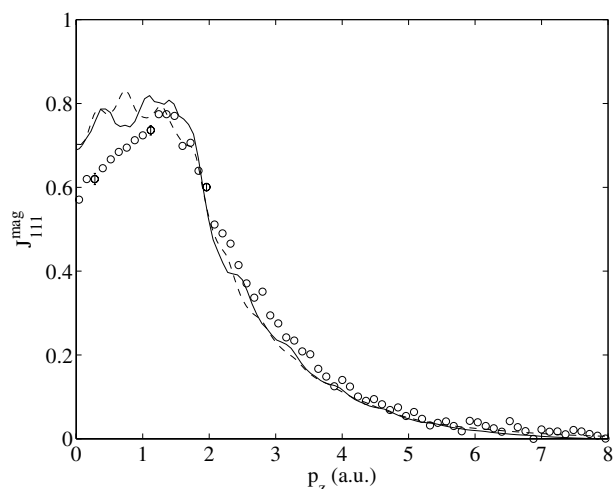


Figure 7. MCP along the [111] direction from the ordered LMTO (solid curve) and disordered KKR-CPA (dashed curve) calculations. The experimental data [10] for the disordered alloy are shown (open circles) with illustrative error bars. The calculations have not been convoluted with the experimental resolution function.

(as expected), can be seen. The agreement with experiment is in general good (for a comparison with the convoluted theoretical profiles, see [10]), but worst in the low-momentum region. There are no experimental data for the [100] direction, which is unfortunate as this direction shows the most structure; periodic signatures of the FS can be seen extending out to 6 au in the ordered calculation.

While it is clear that the shapes of the calculated magnetic profiles do differ for ordered and disordered Fe₃Pt, these differences are unlikely to be resolved in a typical magnetic Compton scattering experiment where the resolution FWHM is ~ 0.4 au (which is almost half the size of the simple cubic BZ). This is indeed the case for the current experimental results, as can be seen in figure 8, where a comparison between MCPs measured along the [110] and [111] directions in the ordered and disordered alloys is shown [10]. However, high-resolution magnetic Compton measurements using a scanning spectrometer rather than a solid-state Ge detector, could reveal both the structure present in the calculated MCPs (especially along the [100] direction), and possibly the difference between the ordered and disordered alloy. Along with such experiments, positron annihilation measurements of the FS could be a more stringent test of our ability to understand the electronic ground state of Fe₃Pt. In particular the question of the dispersion of the flat majority band with respect to the Fermi energy, which differs between the KKR and LMTO calculations for ordered Fe₃Pt, should be resolved by a measurement of the FS topology.

4. Conclusion

First-principles calculations are presented of the electron momentum distributions of the invar alloy Fe₃Pt in ordered and disordered phases using a combination of LMTO, KKR and KKR-CPA methods. Calculations are made of spin densities that are accessible through magnetic Compton scattering measurements. The magnetic properties are found to be fairly robust against using different calculational methods and against choosing the ordered and disordered

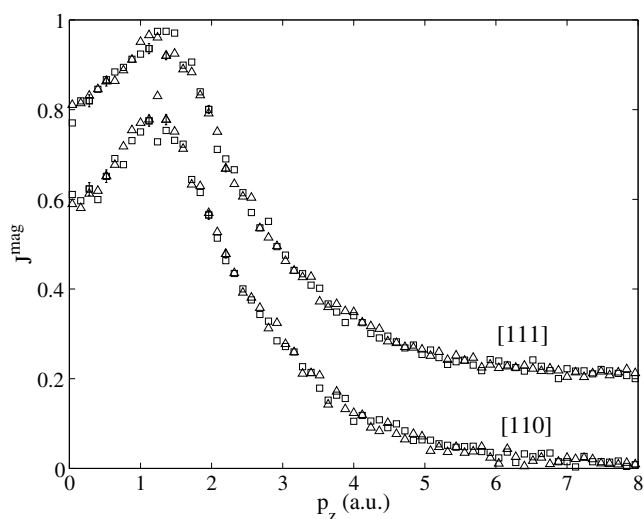


Figure 8. Experimental MCPs in the ordered (Δ) and disordered (\square) alloy resolved along the [110] (bottom) and [111] (top) directions [10]. The two profiles along the [111] direction are offset from zero for clarity.

phases. However, there are differences in the electronic structure and particularly the FS topologies of the ordered and disordered alloys that could be clarified by high-resolution magnetic Compton scattering or positron annihilation experiments.

Acknowledgments

The authors would like to thank the EPSRC (UK) and the Istituto Nazionale di Fisica della Materia (PAIS ELMAMES) (Italy) for financial support. One of us (SBD) acknowledges generous support from the Royal Society. We would also like to thank J W Taylor and J A Duffy for making their experimental data available to us.

References

- [1] Guillaume C E 1897 *C. R. Acad. Sci., Paris* **125** 235
- [2] Weiss R J 1963 *Proc. Phys. Soc. London* **82** 281
- [3] Williams A R, Morruzzi V L, Gelatt C D, Kübler J and Schwarz K 1980 *J. Appl. Phys.* **53** 2019
Moroni E G and Jarlborg T 1990 *Phys. Rev. B* **41** 9600
- [4] Uhl M, Sandratskii L M and Kübler J 1994 *Phys. Rev. B* **50** 291
- [5] van Schilfgaarde M, Abrikosov I A and Johansson B 1999 *Nature* **400** 46
- [6] Wildes A and Cowlam N, private communication in [10]
- [7] Kakeshita T, Takeuchi T, Fukuda T, Tsujiguchi M, Saburi T, Oshima R and Muto S 2000 *Appl. Phys. Lett.* **77** 1502
- [8] Wassermann E F 1991 *J. Magn. Magn. Mater.* **100** 346
- [9] Srajer G, Yahnke C J, Haeflner D R, Mills D M, Assoufid L, Harmon B N and Zuo Z 1999 *J. Phys.: Condens. Matter* **11** L253
- [10] Taylor J W, Duffy J A, Bebb A M, McCarthy J E, Lees M R, Cooper M J and Timms D N 2002 *Phys. Rev. B* **65** 224408
- [11] Wakoh S, Tokii M, Matsumoto M and Matsumoto I 2002 *J. Phys. Soc. Japan* **71** 1393
- [12] Inoue J and Shimizu M 1983 *J. Phys. F: Met. Phys.* **13** 2677
- [13] Hasegawa A 1985 *J. Phys. Soc. Japan* **54** 1477

- [14] Podgórný M 1991 *Phys. Rev. B* **43** 11300
- [15] Podgórný M 1992 *Phys. Rev. B* **46** 6293
- [16] Hayn R and Drchal V 1998 *Phys. Rev. B* **58** 4341
- [17] Sakai N 1996 *J. Appl. Crystallogr.* **29** 81
Cooper M J 1997 *J. Radiat. Phys. Chem.* **50** 63
- [18] Matsui M, Adachi K and Asano H 1981 *Sci. Rep. Res. Inst. Tokohu Univ. (Suppl. 1)* **A 29** 61
Sumiyama K, Shiga M and Nakamura Y 1983 *J. Magn. Magn. Mater.* **31–34** 111
- [19] Andersen O K 1975 *Phys. Rev. B* **12** 3060
Jarlberg T and Arbman G 1977 *J. Phys. F: Met. Phys.* **7** 1635
- [20] Bruno E and Ginatempo B 1997 *Phys. Rev. B* **55** 12946
- [21] Gunnarsson O and Lundqvist B I 1976 *Phys. Rev. B* **13** 4274
- [22] von Barth U and Hedin L 1972 *J. Phys. C: Solid State Phys.* **5** 1629
- [23] Singh A K and Jarlberg T 1985 *J. Phys. F: Met. Phys.* **15** 727
- [24] Poulter J and Staunton J 1988 *J. Phys. F: Met. Phys.* **18** 1877
- [25] Landolt H and Börnstein R 1992 *Numerical Data and Functional Relationship in Science and Technology (Landolt–Börnstein New Series Group III)* vol 19a, ed O Madelung (Berlin: Springer)
- [26] Moroni E G and Jarlberg T 1992 *Structural and Phase Stability of Alloys* ed J L Morán-López *et al* (New York: Plenum) p 103
- [27] Barbiellini B, Moroni E G and Jarlberg T 1991 *Helv. Phys. Acta* **64** 164
- [28] Carbone C, Kisker E, Walker K-H and Wassermann E F 1987 *Phys. Rev. B* **35** 7760
- [29] Bruno E, Ginatempo B, Giuliano E S, Ruban A V and Vekilov Y K 1994 *Phys. Rep.* **249** 353
- [30] Kästner J, Petry W, Shapiro S M, Zheludev A, Neuhaus J, Roessel Th, Wassermann E F and Bach H 1999 *Eur. Phys. J. B* **10** 641
- [31] Wilkinson I, Hughes R J, Major Zs, Dugdale S B, Alam M A, Bruno E, Ginatempo B and Giuliano E S 2001 *Phys. Rev. Lett.* **87** 216401
- [32] Lee Y, Rhee J Y and Harmon B N 2002 *Phys. Rev. B* **66** 054424
- [33] Ito Y, Sasaki T and Mizoguchi T 1974 *Solid State Commun.* **15** 807
- [34] Caporaletti O and Graham G M 1980 *J. Magn. Magn. Mater.* **22** 25